08,11

Calculation of the dynamics of the amorphous phase-crystal interface during solid-phase explosive crystallization

© A.A. Chevrychkina, N.M. Bessonov, A.L. Korzhenevskiy

Institute of Problems of Mechanical Engineering, Russian Academy of Sciences,
St. Petersburg, Russia

E-mail: alekorzh@mail.ru

Received July 5, 2021
Revised July 10, 2021
Accepted July 10, 2021

The nonlinear differential equation described a dynamics of solid-phase explosive crystallization front in a much larger parameters domain in comparison with the theoretical results available in literature was obtained. The features of the self-oscillating mode transition of the front motion to the mode of its self-propagation with a constant velocity was numerically studied in detail.

Ketwords: Explosive crystallization, self-oscillations of the interface glass-crystal, self-propagating front.

DOI: 10.21883/PSS.2022.13.52323.162

1. Introduction

The dynamics of explosive crystallization (EC) occupies a special place in the kinetics of various fronts of physical or chemical nature, such as crystal growth faces, interphase boundaries during phase transitions, magnetic or ferroelectric domain walls, etc. The study of EC in amorphous phase crystallization is important, because the underlying positive feedback between the latent heat release and the front velocity plays a key role and in many other phenomena, that are more difficult to describe quantitatively, for example, in autocatalytic exothermic chemical reactions or the interaction of competing phase transitions in self-propagating high-speed synthesis [1–3]. At the same time, despite the qualitative similarity with some other diffusion-controlled processes, for example, with rapid directional solidification of liquid alloys, a more detailed analysis of EC also indicates the differences in their mathematical description.

In early theoretical studies, the EC analysis was carried out under the assumption of a constant front velocity [4–6], see also review [7]. It was shown that for self-propagating EC fronts, their velocity is determined by the heat balance condition, which at certain parameters values allows for a non-unique solution [5–7]. The discovery of this circumstance made it possible to predict the possibility of thermal hysteresis not only in the constant front velocity approximation, but also in more general cases, however, fundamentally limited by the requirement of quasi-stationarity of mode, see, for example [8].

Experimentally EC was observed in films of a number of pure elements and chemical compounds belonging to materials of various classes. At the same time the typical features of the phenomenon observed on sufficiently large spatial scales and times were identified: the threshold character of the occurrence and suppression of EC, its dependence on the substrate temperature, amorphous film thickness, the method of its preparation, thermal properties of the substrate material, etc. It was found that, depending on the experimental conditions, EC can take place both in the hardness-retaining material and with the formation of an intermediate liquid phase. In addition, the process kinetics can be accompanied by the nucleation of many crystallites in an amorphous matrix or be realized by the spread of a single glass-crystal front, see, for example, [9–15].

Special attention was drawn to the experiments, in which post mortem periodic changes in amorphous films thickness and specific grain sizes in polycrystalline products EC [16] were observed. To explain these effects, an assumption was made, that they are a consequence of periodic oscillations of the front velocity [6]. The possibility of the occurrence of such oscillations was demonstrated within the framework of the analysis of linear stability of the uniform motion of plane fronts [6,17–19]. In subsequent theoretical studies, their nonlinear mode of motion was also studied for both self-propagating EC fronts and under the conditions of weak support of their motion by a mobile heat source (usually a scanning laser beam [17,20,21]). It should be noted, however, that the methods used to derive formulas are rather complicated, the formulas obtained themselves are very cumbersome and, moreover, are applicable only in very narrow ranges of parameter values, that complicates and greatly restricts their practical application. In its turn, numerical calculations performed within the framework of widely used phase field method, see, for example, [22–24] or by molecular dynamics method [25–27], are effective only for describing EC features in models of specific glasses, but do not allow generalizing predictions.

In recent years significant progress has been made in the experimental possibilities of observing in situ the processes accompanying EC. It is primarily associated with the development of a new procedure (dynamic transmission

electron microscopy), with the help of which it was possible to achieve a much higher spatial and temporal resolution of the structure of the crystallizing material [28–30]. In particular, remarkable experiments in [28–30] have shown that the transition of the amorphous state into Ge crystal occurs according to lateral growth mechanism, and not according to the considered in theoretical studies [5,6,17–21] normal growth. This means that first a local crystallized protrusion appears on the front, which then expands and covers the entire front surface. In this case, there can be several protrusions, they expand in an independent way, that clearly indicates the nucleation nature of the process.

On the whole we can be say that the currently accumulated various experimental material about EC exceed the available theoretical results. There is an urgent need to develop new methods for quantitative theoretical calculations both within the framework of traditional general macrokinetic models with a simple EC front geometry and for the models operating on nanoscales.

The purpose of this article is to propose, within the framework of the traditional phenomenological approach, a new theoretical method for calculating the EC front dynamics, which is both simpler and at the same time allowing to describe it in a much wider range of parameters than it was done in [17,20,21]. In this case the main attention will be paid to the calculation of the self-oscillating front dynamics and its transformation into a self-sustaining mode.

2. Model formulation and initial equations

In the basic macrokinetic model EC front is considered as an infinitely thin heat source, which dependence of the velocity on its temperature contains an exponential Arrhenius factor. The heat exchange process in the material volume is described with a standard heat conductivity equation, and the heat sink from the film to the substrate is considered in the relaxation or diffusion mode [7,31]. Since in recent years there is a growing interest in EC in increasingly thin amorphous films, in our article we will consider the first of these modes. In this case the heat problem can be solved in the approximation of a one-dimensional model, in which the heat sink law in the simplest case is assumed to be Newtonian. When the substrate temperature T_S is not high enough and EC process is realized with the support of a scanning laser beam, then the heat conductivity equation contains an additional source. In the result the model equations are as follows:

$$\frac{\partial T}{\partial t} = D\,\frac{\partial T}{\partial z^2} - \Gamma(T - T_S) + J, \tag{1}$$

$$J(z,t) = q_0 V \delta(z - Z(t)) + P(z - V_L t), \tag{2}$$

$$V(T_i) = V_0 \exp\left(-\frac{E}{T_i}\right), \tag{3}$$

where D — the thermoconductivity coefficient, the coefficient Γ sets the rate of heat sink to the substrate, $q_0 = L/c$, L — crystallization heat, c — the heat absorptive capacity, $V = \dot{Z}$ — front velocity, $Z(t)$ — its coordinate, $\delta(z - Z(t))$ — Dirac delta function, $P(z - V_L t)$ function describes heat component from laser illumination, V_L — set laser beam velocity, T_i — front temperature, V_0 — phenomenological parameter, E — effective activation energy.

3. Derivation of front movement equation in differential form

The dynamics of the front coordinate $Z(t)$ is determined from the condition of self-consistent equality of the front temperature $T_i(V)$, taken from formula (3), rewritten in the form of

$$T_i(V) = -\frac{E}{\ln\left(\frac{V}{V_0}\right)} \tag{4}$$

and found from the solution of equation (1). Since this equation is linear, its solution can be written as Green's function convolution $G(z,t)$ with the source $J(z,t)$ in (2). And to obtain the results in an analytical form, it is convenient to write the Green's function $G(z,t)$ using its spatial Fourier transform

$$G(z,t) = \int\limits_{-\infty}^{+\infty} \frac{dk}{2\pi} \exp\left[\left(-Dk^2 - \Gamma\right)t + ikz\right], \tag{5}$$

then use (5) in the equation for solution (1) on the front in the experimentally significant, stationary at large times, mode

$$T(Z(t),t) = T_S + I_1 + I_2,$$

$$I_1 = q_0 \int\limits_{-\infty}^{t} dt' \int\limits_{-\infty}^{+\infty} dz' G(Z(t) - z', t - t') V(t') \delta(z' - Z(t')),$$

$$I_2 = \int\limits_{-\infty}^{t} dt' \int\limits_{-\infty}^{+\infty} dz' G(Z(t) - z', t - t') P(z' - V_L t')). \tag{6}$$

The components I_1 and I_2 in the equation (6), due to the release of crystallization heat and laser illumination, should be calculated separately. The first of them can be represented as the following series:

$$I_1 = q_0 \int\limits_{-\infty}^{t} dt' V(t') G(Z(t) - Z(t'))$$

$$= q_0 \int\limits_{-\infty}^{t} dt' \left[V(t) + \dot{V}(t)(t' - t) + \ldots\right]$$

$$\times \int\limits_{-\infty}^{+\infty} dk \left[1 - ik\,\frac{\dot{V}(t)}{2}(t' - t)^2 - ik\,\frac{\ddot{V}(t)}{6}(t' - t)^3 + \ldots\right]$$

$$\times \exp\left[Dk^2 - ikV(t)\right](t' - t). \tag{7}$$

Since the velocity $V(t)$ and its derivatives are included in (7) only as parameters, it is possible to explicitly integrate over the time t' in all members of the series, although the front dynamics has not been determined yet. Then the k integrals are easily taken from the residues, and it is easy to write down the result in a compact form

$$I_1 = q_0\sqrt{B} \times \left\{1 - \beta\left(1 - \frac{3}{2}\beta\right)\ddot{Z}(t) + \beta^2\left(\frac{3}{2} - \frac{5}{2}\beta\right)\dddot{Z}(t) + \ldots\right\}, \tag{8}$$

where $\beta(V)$ function is determined as

$$\beta(V) \equiv \frac{V^2}{V^2 + 4\Gamma D}, \quad \beta_L \equiv \beta(V = V_L). \tag{9}$$

If the speed of laser beam movement V_L is constant, then the component of illumination I_2 into the value T_i can be written as a source convolution $P(z - V_L t)$ with Green's function G_s of steady-state heat conductivity equation.

$$I_2 = \int_{-\infty}^{+\infty} G_S(Z(t) - z')P(z')\,dz', \tag{10}$$

$$G_S(Z) = \frac{\sqrt{\beta_L}}{V_L}\exp\left[-\frac{V_L\left(z + \beta_L^{-\frac{1}{2}}|z|\right)}{2D}\right], \tag{11}$$

In case when the crystallization front is outside the laser spot, this component exponentially decreases as far as the distance from front to spot increases.

Equating the temperature values on the front T_i in (4) and (6), taking into account (8) and (10), we obtain an equation describing the dynamics of the front coordinate $Z(t)$ in the form of a nonlinear differential equation of infinite order

$$T_S + q_0\sqrt{\beta}\left\{1 - \beta\left(1 - \frac{3}{2}\beta\right)\ddot{Z}(t) + \beta^2\left(\frac{3}{2} - \frac{5}{2}\beta\right)\dddot{Z}(t) + \ldots\right\} + I_2(Z_S)\exp\left[-\frac{V_L(Z - Z_S)}{2Dl}\right] = -\frac{E}{\ln\left(\frac{V}{V_0}\right)}, \tag{12}$$

where the length l is defined by the equation $l^{-1}(V_L) \equiv 1 + \beta_L^{-\frac{1}{2}}$.

In equation (12) $Z_s = V_L t + Z_0$, where Z_0 is the distance between the laser spot and the front position in case of its uniform motion with the velocity V_L. Accordingly, the value Z_0 is determined by the condition

$$T_s + q_0\sqrt{\beta_L} + I_2(Z_s) = -\frac{E}{\ln\left(\frac{V_L}{V_0}\right)}. \tag{13}$$

The advantages of writing the left-hand side of equation (12) in differential form in comparison with the integral in (6) lie in the possibility of constructing approximate solutions (12) in an analytical form and their clear physical interpretation. The next section is devoted to these questions.

4. Steady-state and self-oscillating modes of front dynamics

Obviously, the front velocity in stationary modes, the implementation of which requires laser support, is equal to V_L. In the case of self-propagating EC fronts, it is determined by the stable solution V_s of the equation (13), in which the term I_2 is omitted. It is more convenient to analyze the general properties of equations (12), (13) containing several dimensional parameters, if we go over to dimensionless variables. Therefore, we introduce new time and length as

$$t \to \frac{2D}{V_L^2}t, \quad Z \to \frac{2D}{V_L}Z. \tag{14}$$

In addition to the parameter β introduced above, we will use two more dimensionless parameters, α and R, which are given by the relations

$$\alpha \equiv \frac{q_0}{E}\sqrt{\beta_L}\ln^2\left(\frac{V_L}{V_0}\right), \quad R \equiv \frac{I_2}{q_0 l\sqrt{\beta_L}}. \tag{15}$$

Taking into account that even in the case when equation (13) has a solution with a constant velocity, it may turn out to be unstable, we also introduce the dimensionless deviation of the front coordinate from its value in the stationary mode $h(t) = Z(t) - Z_s$.

We now write the difference between equations (12) and (13) in the introduced dimensionless variables and parameters

$$\sum_{n=2}^{\infty} M_n\frac{d^n h}{dt^n} + M_1\dddot{h} + M_0\ddot{h} + F(\dot{h}) + g\left[\exp\left(-\frac{h}{l}\right) - 1\right] = 0, \tag{16}$$

where

$$M_1(\dot{h}) = \frac{\beta^{\frac{5}{2}}(\dot{h})}{(\dot{h} + 1)^6}\left(\frac{3}{2} - \frac{5}{2}\beta(\dot{h})\right), \tag{17}$$

$$M_0(\dot{h}) = \frac{\beta^{\frac{3}{2}}(\dot{h})}{(\dot{h} + 1)^3}\left(\frac{3}{2}\beta(\dot{h}) - 1\right), \tag{18}$$

$$F = \sqrt{\beta(\dot{h})} - \sqrt{\beta_L}\left[1 + \frac{1}{\alpha}\frac{\ln\left(\frac{V_L}{V_0}\right)\ln(\dot{h} + 1)}{\ln\left(\frac{V_L}{V_0}\right) + \ln(\dot{h} + 1)}\right], \tag{19}$$

$$g = Rl\sqrt{\beta_L}, \tag{20}$$

$$\beta(\dot{h}) \equiv \frac{(1 + \dot{h})^2}{(1 + \dot{h})^2 + \left(\frac{1}{\beta_L} - 1\right)}. \tag{21}$$

Hypermasses M_n at $n > 1$ can be calculated in the same way as it was done for M_0 and M_1.

Note that it is useful to interpret the equation (16) as the fulfillment of a balance of forces, including hyperinertial forces (arising due to delay, like in the classical setting of the problem relating to selfretardation of a non-point model electron), inertial force, nonlinear viscous friction force, and restoring force.

Now let us show, that at small values of the dimensionless parameter g (i.e. at sufficient weak laser support of front motion), self-oscillatory solutions with good accuracy can be found by solving the equation for a nonlinear oscillator:

$$M_0(\dot{h})\ddot{h} + F(\dot{h}) + g[\exp(-h/l) - 1] = 0. \qquad (22)$$

It is clear from (18) that, in general, any oscillatory solutions of equation (22) exist only under the condition $\beta < 2/3$ (i. e. in the presence of a sufficiently large heat removal to the substrate, that is typical of very thin films), when the sign M_0 matches the restoring force sign. Note that, compared to the similar problem of rapid directional crystallization (RDS) of [32–34] alloy, this „restoring" force in (22) is negative, that is a consequence of the typical of EC process positive feedback due to another in comparison with the FDC temperature gradient sign.

Whether oscillatory solutions (22) are self-oscillating depends at $g \ll 1$ on the derivative sign of „friction force" F (taken at $V = V_L$). From (19) we find on the plane $\alpha - \beta$ the line of sign change $dF/d\dot{h}$ (at $V = V_L$):

$$\frac{1}{2}\frac{\beta'}{\beta} V_L - \frac{1}{\alpha} = 0 \qquad (23)$$

or equivalent

$$\beta = \frac{\alpha - 1}{\alpha}. \qquad (24)$$

This line with the accuracy up to $O(g)$ coincides with the Hopf bifurcation line of the stationary front motion

$$\beta = \frac{\alpha - 1}{\alpha} + \frac{M_1}{M_0} R = \frac{\alpha - 1}{\alpha} + \frac{(\alpha - 1)(2\alpha - 5)}{\alpha(3 - \alpha)} R. \quad (25)$$

It is obtained at $\dot{h}$ linearization of equation (16), in which the component of the first term (sum) is omitted, which gives a higher order correction $O(g^2)$. This position of the instability line confirms the usefulness of the above physical interpretation.

Line crossing (25) towards larger values α results in the appearance of a stable cycle. Small oval cycles appear in the immediate vicinity of it, and velocity fluctuations $\dot{h}(t)$ are close to harmonic ones, see Fig. 1.

When deepening into the instability zone, the cycles quickly lose their oval shape, see Fig. 2, and oscillations acquire a pronounced relaxation character, see Fig. 3.

As we continue to move deeper into this zone, two possible scenarios arise. In one scenario the periodic front motion occurs with its stops. Equation (22) makes allows to establish the fact of only the first stop, see Fig. 4, since derivation of equation (22) assumes that the average motion velocity is equal to the velocity V_L, and the presence of stops results in lower average speeds.

Another scenario is associated with a significant nonlinearity of the restoring force in (22), see Fig. 5, and the appearance of an additional zero in the function $F(\dot{h})$. This situation is illustrated by Fig. 6, which shows that the point $\dot{h} = 0$ corresponding to „laser" mode with $V = V_L$ becomes unstable $F' > 0$ (while additional zero for $\dot{h} > 0$ (i. e. $V > V_L$) is stable ($F' < 0$)) and, therefore, the front runs away from the laser spot, and the EC goes into a self-sustaining mode.

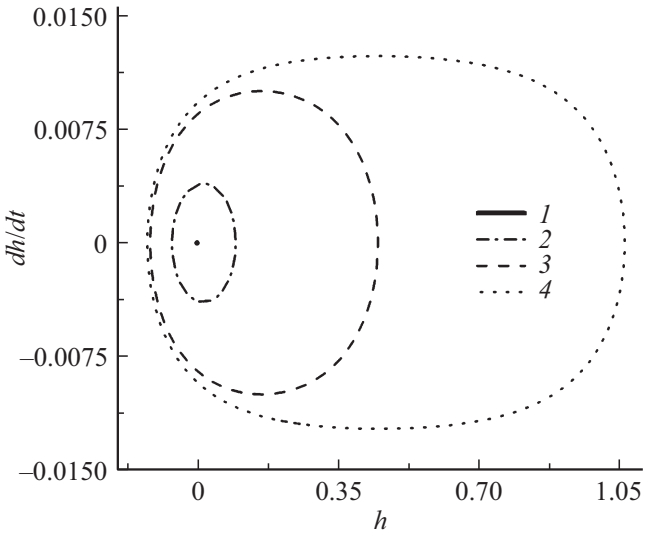

Figure 1. Stable oval cycles in the immediate vicinity of the instability line (25). Values of parameters $R = 10^{-4}$, $\beta = 0.04$, $\ln\left(\frac{V_L}{V_0}\right) = -3$, line *1* — $\alpha = 1.041666$, line *2* — $\alpha = 1.041668$, line *3* — $\alpha = 1.041675$, line *4* — $\alpha = 1.0416782$.

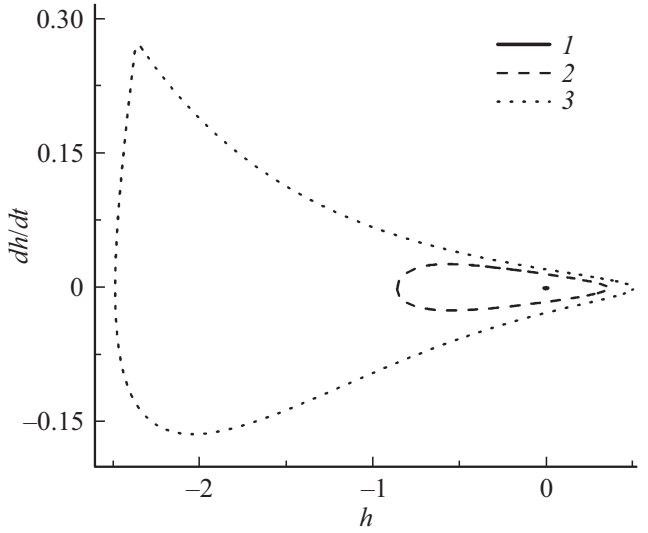

Figure 2. Cycles of quasi-harmonic (line *2*) and relaxation oscillations (line *3*). Values of parameters $\beta = 0.55$, $\ln\left(\frac{V_L}{V_0}\right) = -20$, $R = 10^{-4}$, line *1* — $\alpha = 2.222$, line *2* — $\alpha = 2.223$, line *3* — $\alpha = 2.2625$.

The table shows the runaway front velocities obtained by direct numerical solution of equation (22) (left column) and the positions of function $F(\dot{h})$ zeros (right column).

Taking into account that the numerical solution in some cases might not yet reach the asymptotics, it can be

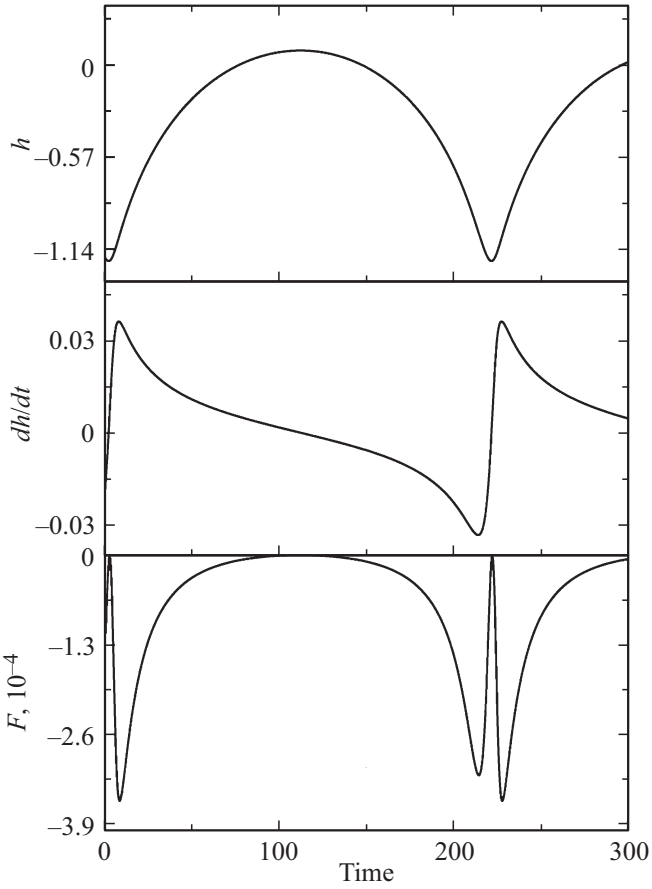

Figure 3. Relaxation oscillation mode. The dependence of „viscous force" $F(\dot{h})$ is defined by relation (19). The values of parameters $\beta = 0.6$, $\ln\left(\frac{V_L}{V_0}\right) = -2$, $R = 10^{-4}$, $\alpha = 2.5006$.

considered established that the velocity of the self-sustaining front $V_s = 1 + \dot{h}$ is set by zero $F(\dot{h})$.

Our numerical calculations also show that for the same values of the problem parameters, but different selection of

Comparison of zeros of function F set by the formula (19) and a runaway mode of equation (22)

β_L	$\alpha = \frac{1.01}{1-\beta_L}$	Zeroes of function F(19)	$\dot{h}$ in runaway mode from solution of equation (22)
0.02	1.03	3.04	3.03
0.03	1.04	2.25	2.24
0.04	1.05	1.72	1.69
0.05	1.06	1.33	1.29
0.06	1.07	1.03	0.976
0.07	1.09	0.81	0.863
0.08	1.100	0.63	0.66
0.09	1.11	0.49	0.49
0.011	1.02	4.2	4.19
0.012	1.022	4.04	4.03
0.013	1.023	3.89	3.88

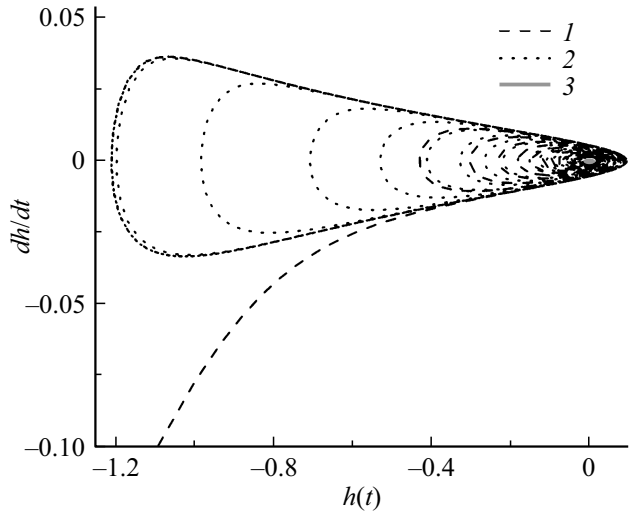

Figure 4. Front stop ($\dot{h} \to -1$ for line *1*). The values of parameters $\beta = 0.6$, $\ln\left(\frac{V_L}{v_0}\right) = -2$, $R = 10^{-4}$, line *1* — $\alpha = 2.5007$, line *2* — $\alpha = 2.5006$, line *3* — $\alpha = 2.5$.

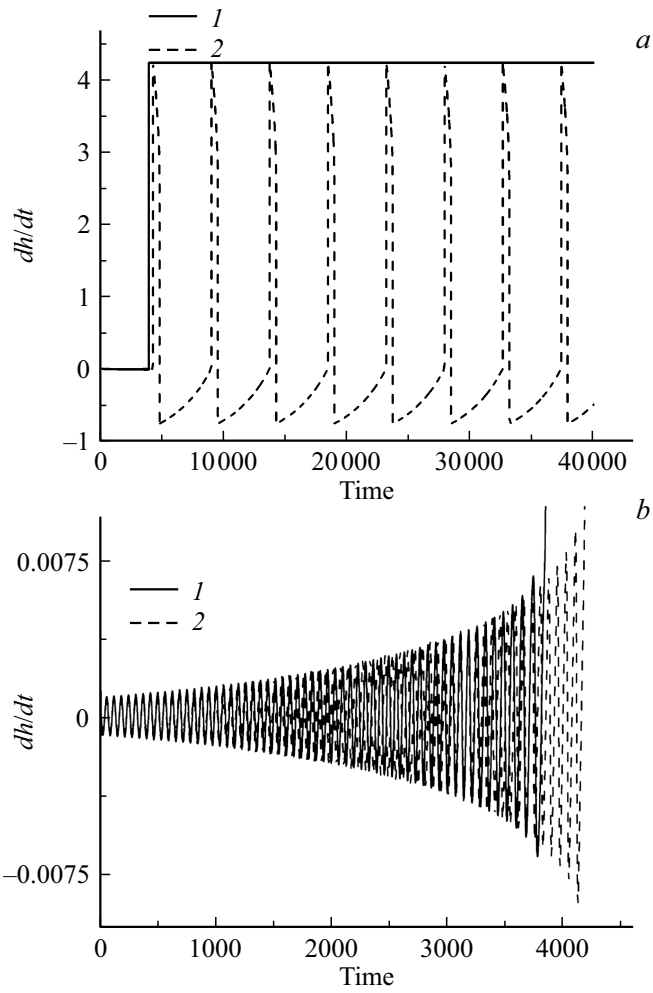

Figure 5. Illustration of the importance of restoring force non-linearity. Values of parameters $\beta = 0.001$, $R = 0.0001$, $\ln\left(\frac{V_L}{V_0}\right) = -3$, $\alpha = 1.01011$. Line *1* — equation (22), line *2* — equation (22) with linear approximation of the restoring force. *a*) extended period of time; *b*) initial period of time.

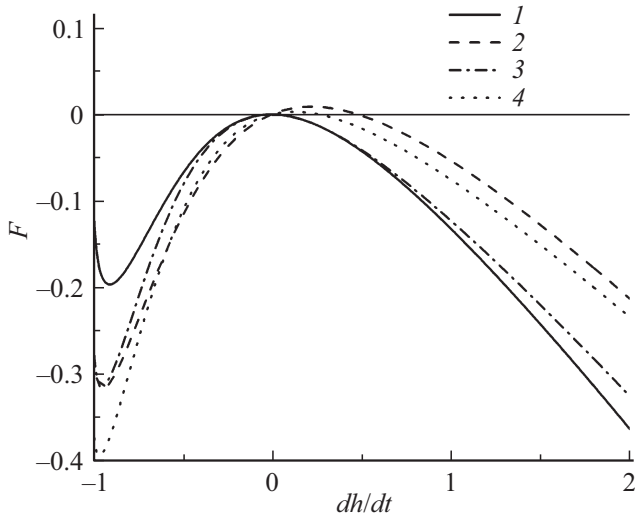

Figure 6. Dependence (19). Values of parameters $\ln\left(\frac{V_L}{V_0}\right) = -3$, line *1* — $\beta = 0.55$, $\alpha = 2.22$, line *2* — $\beta = 0.55$, $\alpha = 3$, line *3* — $\beta = 0.65$, $\alpha = 2.85$, line *4* — $\beta = 0.65$, $\alpha = 3.5$.

the initial values $h(t = 0)$, $\dot{h}(t = 0)$, a change of the dynamic mode is possible. In this regard, we should note that the initial value of the front velocity can be set by starting the experiment with a short laser pulse from $I_2 = f\delta(t)$, which will result in a jump in velocity$V_0 \approx \frac{f}{M_0}\Delta t$, provided that the pulse duration $\Delta t \gg \frac{M_1}{M_0}$. Thus, you can control the initial selection of the mode or switch it over during the EC process.

5. Conclusion

The study offers an analytical method of EC front dynamics calculation using the solution of the derived by us approximate nonlinear differential equation. The method is applicable in a much wider range of parameters in comparison with theoretical results available in the literature. Thus, the results of [17] are applicable only in the vicinity of an isolated point with coordinates $\beta = 2/3$, $\alpha = 3$. In the study [20] the differential equation describing the front dynamics was derived only for the case of small amplitudes of velocity oscillations, while proposed by us method is free from this limitation. In addition, in our study we numerically studied in detail the special features of front motion self-oscillating mode transition to the mode of its self-propagation at constant velocity. Since the method allows one to reveal the general parametric dependences of the EC regimes, its results are a useful guideline for studies aimed at a more detailed description of EC on meso- and microscopic scales. Note, that the approach used in this study allows taking into account various laser modes. Due to the inclusion of Langevin forces in the derived equation of interphase front motion, this approach can also be used to describe EC mode, in which the nucleation process plays the leading role.

Work funding

This study was financially supported by the Russian Science Foundation (project No. 19-19-00552).

Conflict of interest

The authors declare that they have no conflict of interest.

References

[1] I. Prigozhin, D. Kondepudi. Sovremennaya termodinamika. Ot teplovyh dvigatelej do dissipativnyh struktur. (in Russian) Mir, M. (2002). 461 p.
[2] A.S. Rogachev, S.G. Vadchenko, A.S. Aronin, A.S. Shchukin, D.Yu. Kovalev, A.A. Nepapushev, S. Rouvimov, A.S. Mukasyan. J. Alloys Compd. **749**, 44 (2018).
[3] V.G. Myagkov, A.A. Ivanenko, L.E. Bykova, V.S. Zhigalov, M.N. Volochaev, D.A. Velikanov, A.A. Matsynin, G.N. Bondarenko. Sci. Rep. **10**, *1*, 1 (2020).
[4] G.H. Gilmer, H.J. Leamy. In: Laser and Electron-Beam Processing of Materials/Eds C.W. White, P.S. Peercy. Academic, N.Y. (1980). P. 227.
[5] V.A. Shklovsky. ZhETF (in Russian) **82**, *2*, 536 (1982).
[6] W. van Saarloos, J.D. Weeks. Phys. Rev. Lett. **51**, 1046 (1983).
[7] V.A. Shklovsky, V.M. Kuz'menko. UFN (in Russian) **157**, 311 (1989).
[8] A.V. Koropov, V.A. Shklovsky. Him. Fizika (in Russian) **7**, 338 (1988).
[9] G. Auvert, D. Bensahel, A. Perio, T. Nguyen, G.A. Rozgonyi. Appl. Phys. Lett. **39**, 724 (1981).
[10] H.J. Zeiger, John C.C. Fan, B.J. Palm, R.I. Chapman, R.P. Gale. Phys. Rev. B **25**, 4002 (1982).
[11] D. Bensahel, G. Auvert, A. Perio, J.C. Pfister. J. Appl. Phys. **54**, 3485 (1983).
[12] H.-D. Geiler, E. Glaser, Goetz, M. Wagner. J. Appl. Phys. **59**, 3091 (1986).
[13] C. Grigoropoulos, M. Rogers, S.H. Ko, A.A. Golovin, B.J. Matkowsky. Phys. Rev. B **73**, 184125 (2006).
[14] B.C. Johnson, P. Gortmaker, J.C. McCallum. Phys. Rev. B **77**, 214109 (2008).
[15] K. Ohdaira, H. Matsumura. J. Cryst. Growth **362**, 149 (2013).
[16] C.E. Wickersham, G. Bajor, J.E. Greene. Solid State Commun. **27**, 17 (1978).
[17] W. van Saarloos, J.D. Weeks. Physica D **12**, 29 (1984).
[18] D.A. Kurtze, W. van Saarloos, J.D. Weeks. Phys. Rev. B **30**, 1398 (1984).
[19] I. Smagin, A. Nepomnyashchy. Physica D **238**, 706 (2009).
[20] D.A. Kurtze. Physica D **20**, 303 (1986).
[21] D.A. Kurtze. Phys. Rev. B **40**, 11104 (1989).
[22] N. Provatas, M. Grant, K.R. Elder. Phys. Rev. B **53**, 6263 (1996).
[23] E.J. Albenze, M.O. Thompson, P. Clancy. Ind. Eng. Chem. Res. **45**, 5628 (2006).
[24] C. Reina, L. Sandoval, J. Marian. Acta Materialia **77**, 335 (2014).
[25] V. Turlo, O. Politano, F. Baras. Acta Materialia **120**, 189 (2016).

[26] F. Baras, V. Turlo, O. Politano, S.G. Vadchenko, A.S. Rogachev, A.S. Mukasyan. Adv. Eng. Mater. **20**, *8*, 1800091 (2018).
[27] S.A. Rogachev, O. Politano, F. Baras, A.S. Rogachev. J. Non-Cryst. Solids **505**, 202 (2019).
[28] L. Nikolova, T. LaGrange, M.J. Stern, J.M. MacLeod, B.W. Reed, H. Ibrahim, G.H. Campbell, F. Rosei, B.J. Siwick. Phys. Rev. B **87**, 064105 (2013).
[29] G.C. Egan, T.T. Li, J.D. Roehling, J.T. McKeown, G.H. Campbell. Acta Materialia **143**, 13 (2018).
[30] G.C. Egan, T.T. Rahn, A.J. Rise, H.Y. Cheng, S. Raoux, G.H. Campbell, M.K. Santala. J. Appl. Phys. **126**, 105110 (2019).
[31] C. Buchner, W. Schneider. J. Appl. Phys. **117**, 245301 (2015).
[32] A.L. Korzhenevskii, R. Bausch, R. Schmitz. Phys. Rev. Lett. **108**, 046101 (2012).
[33] A.L. Korzhenevskii, R. Bausch, R. Schmitz. Phys. Rev. E **85**, 021605 (2012).
[34] A.A. Chevrychkina, N.M. Bessonov, A.L. Korzhenevsky. Physics of the Solid State **61**, *11*, 2122 (2019).